Dependence of phonon widths on pressure and isotopic mass: ZnO

J. Serrano[*,1], **F. Widulle**[1], **A. H. Romero**[2], **A. Rubio**[3], **R. Lauck**[1], and **M. Cardona**[1]

[1] Max-Planck Institut für Festkörperforschung, Heisenbergstrasse 1, 70569 Stuttgart, Germany

[2] Advanced Materials Department, IPICyT, 78231 San Luis Potosí, Mexico

[3] Dpto. Física de Materiales, Facultad de Ciencias Químicas, Universidad del País Vasco, Centro Mixto CSIC-UPV/EHU and Donostia International Physics Center, 20018 San Sebastián, Basque Country, Spain

Considerable attention has been devoted recently to the dependence of the widths of the Raman phonons of semiconductors on pressure and on isotopic mass. The dependence on pressure is usually small and monotonic unless the phonon happens to be close to a singularity of the two-phonon density of states (DOS) which determines its width. In the latter case, strong nonmonotonic dependences of the phonon width on pressure and on isotopic mass can appear. We have investigated the E_2^{high} phonons of ZnO crystals with different isotopes and observed a wide range of FWHM depending on isotopic masses. *Ab initio* calculations of the two-phonon DOS provide an explanation for this variation of the FWHM: the E_2^{high} frequency falls on a sharp ridge of the 2-DOS corresponding to combinations of TA and LA phonons. Changes in isotopic mass result in a motion of the E_2^{high} frequency up and down that ridge which produces the changes in FWHM. These phenomena suggest a decrease of the FWHM with pressure which seems to be present in existing data obtained at 300 K. Similar phenomena are discussed for the E_2^{low} phonons. Applications of the isotope and pressure techniques to the elucidation of two-phonon spectra will be presented.

Introduction Since the pioneering work of Weinstein for GaP [1] it is known that the widths and lineshapes of phonons can, in some cases, be strongly modified by application of pressure. The diamond anvil cell is an excellent tool for such investigations [2] which yield detailed information about the anharmonic decay mechanisms responsible for linewidths and lineshapes. The reason for the drastic lineshape changes observed by Raman spectroscopy in CuCl [3], CuBr [4], GaP [5] and, to a lesser extent Si [6] and CuI [7] is that, in these cases, the anharmonic self-energy is determined by decay into two phonons close to Van Hove singularities at the edge of the Brillouin zone. The fact that the corresponding two-phonon density of states (DOS) has strong singularities near Raman LO (CuBr) or TO (CuCl, GaP) phonons, together with strong anharmonic coupling constants, gives rise to complex lineshapes which are determined not only by the imaginary part but also by the real part of the self-energy. Similar effects have been observed for the Raman LO phonons in CuBr. In these examples the application of hydrostatic pressure leads to a "hardening" of the optical modes, which then shift to higher frequencies, and a "softening" of the transverse acoustic (TA) ones.

---

[*] Corresponding author: e-mail: J.Serrano@fkf.mpg.de, Phone: -49-711-689-1737, Fax: -49-711-689-1632
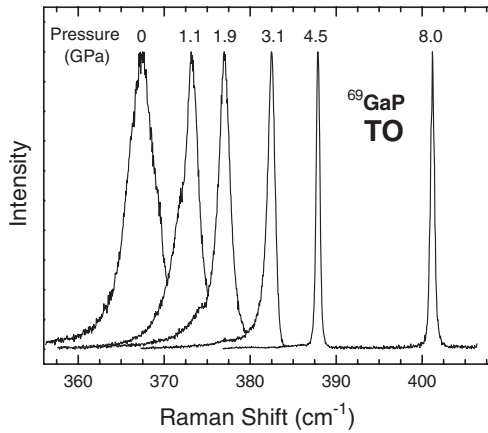
Fig. 1 Raman spectra of the anomalous TO phonons of GaP at different pressures. The TO peak sharpens with increasing pressure due to the different Grüneisen parameters for the Van Hove singularity and the optical phonons. The spectra were reported recently by Ves et al. in [5].

The near-resonance of the Raman mode with a two-phonon state, involving at least a TA mode, can thus be strongly modified by pressure. In the cases just mentioned, the so-called Fermi resonance of the one-phonon with the two-phonon states is offset by the shift of these states in opposite directions, a fact which leads to a decrease in the width of the Raman phonon and the evolution of the lineshape towards a standard Lorentzian. Recent results for GaP [5] are shown in Fig. 1.

Since the fall of the Iron Curtain stable isotopes of many elements which are constituents of the tetrahedral semiconductor crystals have become available at affordable prices. With them, crystals of variable isotopic composition have been grown [9, 10]. Variation of the isotopic composition of a crystal leads to changes in phonon frequencies. Small disorder-induced self-energies may also appear but drastic effects on phonon linewidths are neither expected nor observed. For monatomic crystals (e.g. Si [11]) variation of the mass leads simply to a scaling of the frequency in the dispersion relations within the harmonic approximation. For binary (or even more so for multinary) crystals, isotopic substitution can lead to a non-affine deformation of the dispersion relations and the two-phonon DOS.

The DOS used here is that which corresponds to two-phonons with q-vectors which add up to the q-vector of the decaying phonon whose width is under consideration: $q_0 = q_1 + q_2$; for Raman phonons $q_0 \simeq 0$. At high temperatures two-phonon difference modes, with $q_0 = q_1 - q_2$, may also play a role [12].

As an example we mention GaP and CuCl. For these materials, the Raman frequencies (TO and LO)
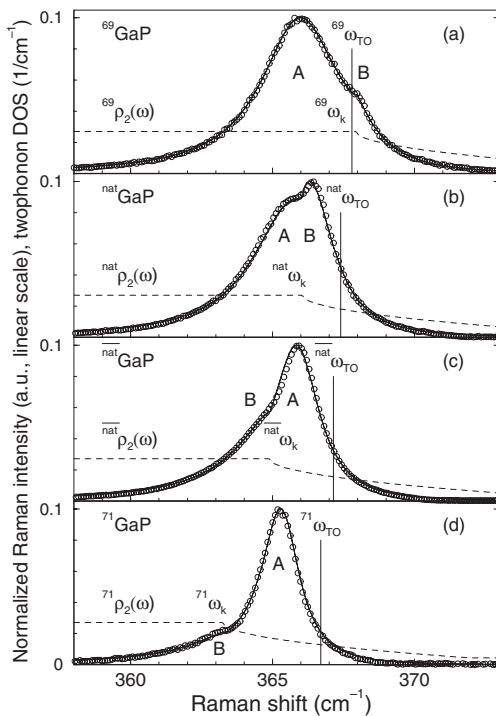
Fig. 2 Low temperature (6 K) Raman spectra of the TO phonons of GaP for different gallium isotopic compositions, reported in [13]. Besides the isotopically pure ^{69}GaP (a) and ^{71}GaP (d), the spectra of natural GaP (^{69}Ga$_{0.6}$^{71}Ga$_{0.4}$P) (b) and its complementary composition (^{69}Ga$_{0.4}$^{71}Ga$_{0.6}$P), denoted by $\overline{\text{nat}}$GaP (c), are also shown. The solid lines are fits to the experimental data (symbols) using the two-phonon DOS, $\rho_2(\omega)$, displayed by the dashed lines. The vertical lines represent the δ-function peaks of the harmonic TO phonons (see Ref. [13] for details).

are mainly determined by the lighter anion mass whereas the TA frequencies at the edge of the Bril-louin zone are determined by the cation mass. By increasing the mass of the cation and decreasing that of the anion, effects on the above mentioned Fermi resonances, qualitatively similar to those induced by a hydrostatic pressure, are produced. We show in Fig. 2 [13] recent measurements of those isotopic effects on the TO Raman phonons of GaP. Notice that the peak sharpens considerably when [69]Ga is replaced by [71]Ga (Fig. 2d), thus simulating the effect of high pressure, Fig. 1, whereas the broadest peak is obtained for [69]GaP when the TO phonon is nearly degenerate with the $(TA + LA)_X$ Van Hove singularity.

Note that in [69]GaP the peak is actually a doublet, corresponding to the strong hybridization of TO with $(TA + LA)_X$. Unfortunately, phosphorus (like aluminum, arsenic and iodine) only has one stable isotope but the gallium substitution suffices to make the point. For similar effects on the TO phonons of CuCl see Figs. 3 and 4 of Ref. [8].

The wurtzite crystal structure is a tetrahedral structure adopted by a number of technologically important binary semiconductors (e.g. GaN, CdS, CdSe, ZnO). It has four atoms per primitive cell, which lead to the doubling of the number of phonons at $q = 0$, thus adding two doubly degenerate Raman active phonons of E_2 symmetry to the IR- and Raman-active LO and TO phonons of the zinc blende structure. The hexagonal crystal field also induces splittings of the TO and LO phonons depending on the direction of vibration with respect to the c-axis and the q-vector. The increase in the number of phonons enhances the possibility of observing "accidental" Fermi resonances with the two-phonon DOS. Nevertheless the investigations of pressure and isotope effects on the lineshapes performed for wurtzite-type materials are rather scarce (ZnO [14, 15], CdS [16], GaN [17]).

In this paper we present Raman spectra measured at 6 K and 300 K for wurtzite ZnO prepared with different zinc ([64]Zn, [68]Zn) and oxygen (^{16}O, ^{18}O) isotopes and also with natural elements. The most interesting effect discovered is a strong dependence of the width of the E_2^{high} peak on the isotopic masses (it varies from 0.8 cm^{-1} to 5 cm^{-1}, FWHM, at 6 K). This effect can be described in terms of a Fermi resonance with the two-phonon DOS. For a quantitative interpretation we have performed an *ab initio* calculation of the lattice dynamics of ZnO because existing inelastic neutron scattering measurements and model calculations are rather unsatisfactory [18–20] (see Fig. 3 and Ref. [21]). The corresponding two-phonon sum and difference DOS have been evaluated. The E_2^{high} phonon appears at the upper flank of a two-phonon sum band, a fact which can account for the measured changes in the E_2^{high} phonon width. These results, and also calculations, suggest that the FWHM of the E_2^{high} phonons of ZnO should decrease with increasing hydrostatic pressure. Recent measurements performed at room
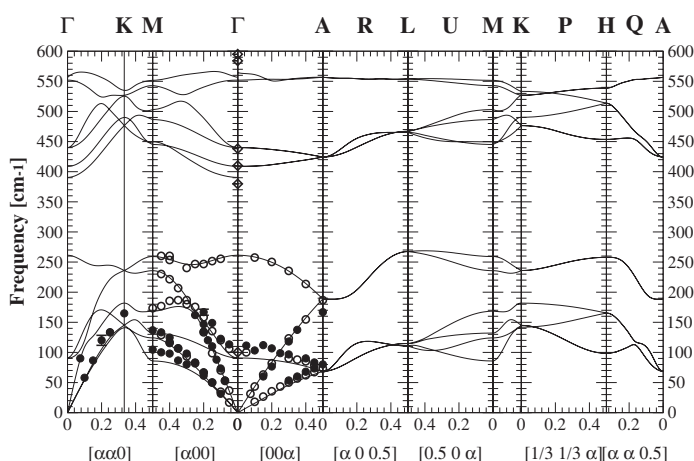
Fig. 3 *Ab initio* phonon dispersion relations calculated for ZnO along directions of high symmetry. The solid and open circles represent inelastic neutron data at room temperature from Refs. [19] and [20], respectively, and the open diamonds represent our Raman data for natural ZnO at 6 K.
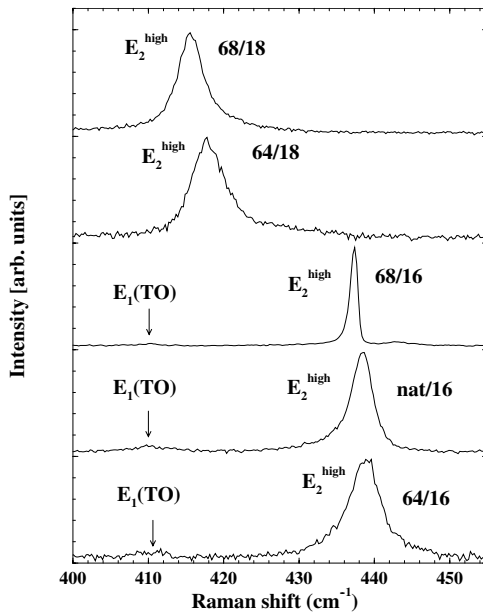
Fig. 4 Raman spectra of the E_2^{high} mode of ZnO for several isotopic compositions measured at 6 K. The different line-width and slight asymmetry observed for each isotopic composition can be explained from the resonance with an edge of the two-phonon (sum) density of states.

temperature [14, 15] qualitatively confirm this conclusion. In order to obtain more quantitative results, pressure measurements on several isotopically modified samples are under way.

Experimental details We performed Raman measurements of ZnO at 6 K and 300 K in samples of several isotopic compositions ($^{nat}Zn^{16}O$, $^{64}Zn^{16}O$, $^{68}Zn^{16}O$, $^{64}Zn^{18}O$, $^{68}Zn^{18}O$). These samples were grown by chemical vapor transport at a source temperature of $\approx 900\,°C$, using ammonium chloride as transport agent. Purification, synthesis, and crystal growth were performed in the same ampoule for small quantities of the materials.

We used for excitation the 676 nm and 406 nm Kr^+ laser lines for low and high temperature measurements, respectively (due to laser availability). The scattered light was analyzed with a triple grating XY Dilor spectrometer operated in the subtractive mode, and detected with a charge-coupled-device (CCD). The Raman signal was calibrated with laser plasma lines which were fitted with a Gaussian, yielding a spectral resolution of 0.6 cm^{-1} and 2.9 cm^{-1}, for 6 K and 300 K, respectively. Several polarization configurations as described in [22] were used to identify the different modes observed in the spectra.
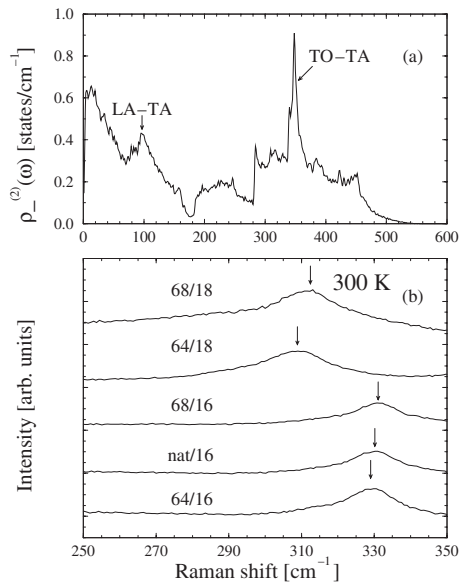
Ab initio calculations The experimental data reported by Raman and neutron scattering for the phonon dispersions of ZnO do not allow the reliable use of semiempirical models to obtain the two-phonon DOS. Therefore, we have undertaken *ab initio* calculations of the phonon dispersion relations of ZnO.

The calculations were performed with the code ABINIT [25], employing pseudopotentials [26] and a plane wave basis, within the framework of density functional perturbation theory. The linear response method [23, 24] was used to obtain the phonon frequencies and eigenvectors. The details of the calculations and a comprehensive report on the lattice dynamics at several pressures will be published elsewhere [21].

We use a cutoff of 60 Hartree in the kinetic energy for the basis expansion, and a $6 \times 6 \times 3$ Monkhorst-Pack grid [27] for integration in reciprocal space. With these parameters, a convergence better than 1 mHartree in the total energy was achieved. We calculated the dynamical matrices for a grid of 14 points in the Brillouin zone. This allowed us to calculate by Fourier transform the interatomic force constants for any arbitrary q-vector, which we used to obtain the two-phonon DOS for both sum $[\rho_+^{(2)}(\omega)]$ and difference $[\rho_-^{(2)}(\omega)]$ processes, needed to analyze the phonon linewidths. Using a conjugate-gradient algorithm, we performed a relaxation of both internal parameters and lattice constants obtaining $a = 3.198$ Å, $c = 5.167$ Å, and $u = 0.379$, in agreement with the reported experimental data: $a_{exp} = 3.249(6)$ Å, $c_{exp} = 5.204(2)$ Å, and $u_{exp} = 0.3819(1)$ [28].

Figure 3 displays the calculated phonon dispersion relations of ZnO along the high symmetry directions. There is good agreement with the Raman and neutron data, represented in the figure by open diamonds and circles, respectively.

Fig. 5 Calculated two-phonon DOS for ZnO at 0 GPa (a). Figure 5b shows a zoom of the region of the E_2^{high} mode where the symbols display the linewidth for several isotopic compositions and their frequencies have been shifted according to $M_{Zn}^{-1/2}$, using ^{68}Zn as a reference, to correct for the shift of the DOS with the isotopic mass, and $\rho_+^{(2)}(\omega)$ has been shifted by $+8 \, cm^{-1}$.

Linewidths of the E_2^{low} and E_2^{high} phonons As a wurtzite crystal, ZnO possesses two Raman active E_2 phonons (E_2^{high} at $\approx 438 \, cm^{-1}$ and E_2^{low} at $\approx 100 \, cm^{-1}$ for natural ZnO at 6 K) [29–31]. The Raman spectra of the E_2^{high} phonons are shown in Fig. 4 for several isotopic compositions.

The frequency shift with Zn isotope is small, whereas that with oxygen isotope is large, a fact which indicates the predominance of oxygen-motion in the corresponding eigenvector. Following Ref. [17], we determined from these shifts the eigenvector components $e_O = 0.65$, $e_{Zn} = 0.27$, in good agreement with the calculations ($e_O = 0.653$, $e_{Zn} = 0.272$). Most striking in this figure is the strong dependence of the linewidth on isotopic composition, from $0.8 \, cm^{-1}$ for ^{68}Zn^{16}O to $5 \, cm^{-1}$ for ^{64}Zn^{18}O. Its origin is illustrated in Fig. 5b, where the two-phonon DOS is plotted multiplied by a fitted factor of 39 which represents an anharmonic coupling constant to the E_2^{high} phonon ($|V_3|^2 = 39 \, cm^{-2}$, see also [8]).

This scaled DOS is meant to represent the linewidths of the E_2^{high} phonons which are displayed by points with the frequency shifted so as to compensate for the shift of the DOS with Zn mass, thus assuming that this does not shift with oxygen mass in the considered region. In this manner, the DOS can be taken to be independent of the isotopic masses and can be shifted rigidly along the frequency scale so as to obtain the best fit to the experimental widths, thus compensating errors in the *ab initio* calculations of the dispersion relations. The overall agreement of the measured widths with the calculated ones is excellent, the coupling constant $|V_3|^2$ being close to that found for the TO phonons of GaP [13].

Figure 5b suggests that a considerable variation of the width should also take place upon application of pressure: The DOS (corresponding to TA + LA phonons) should shift down with pressure while the E_2^{high} frequency should shift up [14, 15]. This should result in a sharpening of the E_2^{high} peak

Fig. 6 Raman spectra of the E_2^{high} phonon of natural ZnO at 300 K displaying the decrease in FWHM with increasing pressure ($7.9 \, cm^{-1}$ at 0 GPa and $5.5 \, cm^{-1}$ at 3 GPa). The data are basically those in Fig. 1 of [14]. We are thankful to A. Polian for an expanded plot of these data and other data in [14].

Fig. 7 (a) Calculated two-phonon difference DOS, $\rho_{-}^{(2)}(\omega)$, and (b) second order band observed in the Raman spectra of ZnO at 300 K for several isotopic compositions (the arrows indicate the position of the maxima). This band does not appear at low temperature and can be attributed to the Van Hove singularity $(TO - TA)$ of $\rho_{-}^{(2)}(\omega)$ located at $\approx 350\ \mathrm{cm}^{-1}$. There is another singularity $(LA - TA)$ at $\approx 100\ \mathrm{cm}^{-1}$ which can explain partially the E_2^{low} phonon linewidth.

with increasing pressure which can be observed, with a trained eye, in Fig. 1 of [14] and of [15], although these data were not obtained with the problem at hand in mind. We have replotted in Fig. 6 the original spectra measured by Decremps et al. [14] for 0 GPa and 3 GPa at 300 K for a natural sample. These data clearly show the sharpening of the E_2^{high} peak with increasing pressure inferred from Fig. 5.

We have tried to investigate possible effects of the isotopic mass on the width of the E_2^{low} phonon without success. This phonon is very sharp, around $0.3\ \mathrm{cm}^{-1}$ FWHM at 300 K [31] and less than $0.1\ \mathrm{cm}^{-1}$ at 6 K (our work). Recent work for the TA phonons of germanium at the edge of the Brillouin zone (FWHM $\approx 0.2\ \mathrm{cm}^{-1}$ at 300 K [12]) show that the width is mainly determined by decay into the difference of two phonons $(TO - LA)$ and should vanish at low temperature. On the basis of the DOS of Figs. 5a and 7a we conjecture that a similar amount of sum and difference processes may determine the rather narrow width of the E_2^{low} phonons. Measurements with different isotopic compositions indicate a contribution of isotope scattering to the linewidth of about $0.05\ \mathrm{cm}^{-1}$ for the E_2^{low} phonons of ZnO.

We show in Fig. 7b a portion of the two-phonon spectrum of ZnO at room temperature which can be attributed to scattering by $TO - TA$ phonon differences since it vanishes at 6 K. This assignment is confirmed by the isotopic substitution: an increase in the oxygen mass should lead to a decrease of the TO frequency, i.e., a decrease of that of the difference peak. An increase in the Zn mass, however, should result in a decrease of the TA frequency, i.e., an increase in the frequency of the difference peak. These conjectures are confirmed by the measured spectra shown in Fig. 7b. This assignment to $TO - TA$ scattering has been confirmed by measurements under pressure: since the TO frequency increases with increasing pressure while that of the TA phonon decreases, the application of pressure results in a strong increase in the frequency of the $TO - TA$ peak; this is in agreement with the large value of the pressure derivative observed in [15], where this mode was assigned to $E_2^{\mathrm{high}} - E_2^{\mathrm{low}}$.

References

[1] B. A. Weinstein, Solid State Commun. **20**, 999 (1976).
[2] B. A. Weinstein and R. Zallen, in: Light Scattering in Solids, Vol. 4 edited by M. Cardona and G. Güntherodt (Springer, Berlin, 1984), pp. 463−527.
[3] C. Ulrich, A. Göbel, K. Syassen, and M. Cardona, Phys. Rev. Lett. **82**, 351 (1999).
[4] F. J. Manjón, J. Serrano, I. Loa, K. Syassen, C. T. Lin, and M. Cardona, Phys. Rev. B **64**, 064301 (2001).
[5] S. Ves, I. Loa, K. Syassen, F. Widulle, and M. Cardona, phys. stat. sol. (b) **223**, 241 (2001).

[6] C. Ulrich, E. Anastassakis, K. Syassen, A. Debernardi, and M. Cardona, Phys. Rev. Lett. **78**, 1283 (1996).

[7] J. Serrano, M. Cardona, T. R. Ritter, B. A. Weinstein, A. Rubio, and C. T. Liu, Phys. Rev. B **66**, 245202 (2002).

[8] A. Göbel, T. Ruf, C.-T. Lin, M. Cardona, J.-C. Merle, and M. Joucla, Phys. Rev. B **56**, 210 (1997).

[9] V. G. Plekhanov, Isotope Effects in Solid State Physics, in: Semiconductors and Semimetals, Vol. 68, edited by R. K. Willardson and E. R. Weber (Academic Press, San Diego, 2001).

[10] C. T. Lin, E. Schönherr, A. Schmeding, T. Ruf, A. Göbel, and M. Cardona, J. Cryst. Growth **167**, 612 (1996).

[11] F. Widulle, T. Ruf, M. Konuma, I. Silier, M. Cardona, W. Kriegseis, and V. I. Ozhogin, Solid State Commun. **118**, 1 (2002).

[12] A. Debernardi, in: Proc. 26th Internat. Conf. Phys. Semicond., Edinburgh (Scotland), 29 July–2 August 2002, (Institute of Physics Publishing, London, in press); cond-mat/0212209.

[13] F. Widulle, T. Ruf, A. Göbel, E. Schönherr, and M. Cardona, Phys. Rev. Lett. **82**, 5281 (1999).

[14] F. Decremps, J. Pellicer-Porres, A. Marco Saitta, J.-C. Chervin, and A. Polian, Phys. Rev. B **65**, 092101 (2002).

[15] F. J. Manjón, K. Syassen, and R. Lauck, Proc. 6th Europ. High Pressure Res. Conf., Santander (Spain), 16–19 September 2001, High Press. Res. **22**, 299 (2002).

[16] J. M. Zhang, T. Ruf, A. Göbel, A. Debernardi, R. Lauck, and M. Cardona, in: Proc. 23rd Internat. Conf. Phys. Semiconductors, Berlin (Germany), 21–26 July 1996, edited by M. Scheffler and R. Zimmermann (World Scientific, Singapore, 1996), p. 201.

[17] J. M. Zhang, T. Ruf, M. Cardona, O. Ambacher, M. Stutzmann, J.-M. Wagner, and F. Bechstedt, Phys. Rev. B **56**, 14399 (1997).

[18] H. Bilz and W. Kress, Phonon Dispersion Relations in Insulators, edited by M. Cardona, P. Fulde, and H.-J. Queisser (Springer-Verlag, Berlin, 1979), p. 119.

[19] A. W. Hewat, Solid State Commun. **8**, 187 (1970).

[20] K. Thoma, B. Dorner, G. Duesing, and W. Wegener, Solid State Commun. **15**, 1111 (1974).

[21] A. H. Romero, to be published.

[22] C. A. Arguello, D. L. Rousseau, and S. P. S. Porto, Phys. Rev. **181**, 1351 (1969).

[23] S. Baroni, S. de Gironcoli, A. Dal Corso, and P. Giannozzi, Rev. Mod. Phys. **75**, 515 (2001).

[24] X. Gonze, Phys. Rev. B **55**, 10337 (1997).

[25] The ABINIT code is a common project of the Université Catholique de Louvain, Corning Incorporation, and other contributors (URL http://www.abinit.org).
     X. Gouze et al., Comp. Mat. Sci. **25**, 478 (2002).

[26] N. Troullier and J. L. Martins, Phys. Rev. B **43**, 1993 (1991).

[27] H. J. Monkhorst and J. D. Pack, Phys. Rev. B **8**, 5747 (1973).

[28] Landolt-Börnstein, Numerical Data and Functional Relationships in Science and Technology, Group III, Vol. 41b, edited by O. Madelung, U. Rössler, and M. Schulz (Springer–Verlag, Berlin, 1999), pp. 95–96.

[29] T. C. Damen, S. P. S. Porto, and B. Tell, Phys. Rev. **142**, 570 (1966).

[30] J. M. Calleja and M. Cardona, Phys. Rev. B **16**, 3753 (1977).

[31] B. H. Bairamov, A. Heinrich, G. Irmer, V. V. Toporov, and E. Ziegler, phys. stat. sol. (b) **119**, 227 (1983).